874 *Chem. Mater.* **2011,** *23,* 874–885
DOI:10.1021/cm102320b

CHEMISTRY OF MATERIALS
Article

Cyclo-biphenalenyl Biradicaloid Molecular Materials: Conformation, Tautomerization, Magnetism, and Thermochromism†

Jingsong Huang,‡ Bobby G. Sumpter,*,‡ Vincent Meunier,§ Yong-Hui Tian,⊥ and Miklos Kertesz*,⊥

‡*Oak Ridge National Laboratory, Bethel Valley Road, Oak Ridge, Tennessee 37831-6493, United States,* §*Department of Physics, Applied Physics, and Astronomy, Rensselaer Polytechnic Institute, Troy, New York 12180-3590, United States, and* ⊥*Chemistry Department, Georgetown University, 37th & O Street, Washington, D.C. 20057-1227, United States*

Received August 12, 2010. Revised Manuscript Received November 7, 2010

Phenalenyl and its derivatives have recently attracted a great deal of interest as a result of a two-electron multicenter (2e/mc) $\pi-\pi$ bonding between two π-stacked phenalenyl units. The 2e/mc bonded π-dimers are close in energy to the σ-dimers of phenalenyl and therefore fickle properties may emerge from bond fluctuation, yielding "smart" π-functional materials. Here, we examine the valence tautomerization of two cyclo-biphenalenyl biradicaloid molecular materials with chair and boat conformations by spin-restricted (R) and unrestricted (U) DFT using the M06 and B3LYP functionals. We found that the chair conformation involves a 2e/4c $\pi-\pi$ bonded structure, whereas the boat conformation involves a 2e/12c $\pi-\pi$ bonded structure on their potential energy surfaces. The global minimum for the chair conformation is the σ-bonded structure, whereas it is the $\pi-\pi$ bonded structure for the boat conformation. The chair conformation exhibits a stepwise [3,3]-sigmatropic rearrangement, and calculations predict a negligible paramagnetic susceptibility near room temperature. In comparison, the paramagnetism of the boat conformation should be observable by SQUID and ESR. According to the energy differences of the respective σ- and π-dimers of the two conformations and the UV−vis calculations, the color of the chair conformation is expected to become darker, whereas that of the boat conformation should become lighter with increasing temperature.

1. Introduction

Phenalenyl π-radical (**1**, Chart 1) is a stable odd alternant hydrocarbon radical that has been known for decades.[1] The high stability of **1** arises from the π-electron delocalization on the singly occupied molecular orbital (SOMO) and it allows **1** to be observed by ESR in solution. However, **1** cannot be isolated because it undergoes σ-dimerization (Scheme 1),[2] as expected for typical radical species. Various phenalenyl-based organic molecular materials have recently prompted a great deal of both experimental[2−6] and theoretical interest,[6−10] as a result of their diverse intriguing properties as shown, e.g., in a wide range of electrical, optical, and magnetic properties.[11] The fascinating molecular and material properties originate from the ability of phenalenyl and its

† Accepted as part of the "Special Issue on π-Functional Materials".

*Corresponding author. E-mail: sumpterbg@ornl.gov; kertesz@georgetown.edu.

(1) (a) Reid, D. H. *Chem. Ind.* **1956**, 1504. (b) Gerson, F. *Helv. Chem. Acta* **1966**, *49*, 1463.
(2) Zheng, S.; Lan, J.; Khan, S. I.; Rubin, Y. *J. Am. Chem. Soc.* **2003**, *125*, 5786.
(3) (a) Bag, P.; Itkis, M. E.; Pal, S. K.; Donnadieu, B.; Tham, F. S.; Park, H.; Schlueter, J. A.; Siegrist, T.; Haddon, R. C. *J. Am. Chem. Soc.* **2010**, *132*, 2684. (b) Sarkar, A.; Pal, S. K.; Itkis, M. E.; Liao, P. H.; Tham, F. S.; Donnadieu, B.; Haddon, R. C. *Chem. Mater.* **2009**, *21*, 2226. (c) Haddon, R. C.; Sarkar, A.; Pal, S. K.; Chi, X. L.; Itkis, M. E.; Tham, F. S. *J. Am. Chem. Soc.* **2008**, *130*, 13683. (d) Pal, S. K.; Itkis, M. E.; Tham, F. S.; Reed, R. W.; Oakley, R. T.; Haddon, R. C. *J. Am. Chem. Soc.* **2008**, *130*, 3942.
(4) (a) Shimizu, A.; Uruichi, M.; Yakushi, K.; Matsuzaki, H.; Okamoto, H.; Nakano, M.; Hirao, Y.; Matsumoto, K.; Kurata, H.; Kubo, T. *Angew. Chem., Int. Ed.* **2009**, *48*, 5482. (b) Iketaki, K.; Kanai, K.; Shimizu, A.; Kubo, T.; Wang, Z. H.; Ouchi, Y.; Morita, Y.; Nakasuji, K.; Seki, K. *J. Phys. Chem. C* **2009**, *113*, 1515. (c) Kubo, T.; Goto, Y.; Uruichi, M.; Yakushi, K.; Nakano, M.; Fuyuhiro, A.; Morita, Y.; Nakasuji, K. *Chem. Asian J.* **2007**, *2*, 1370. (d) Morita, Y.; Aoki, T.; Fukui, K.; Nakazawa, S.; Tamaki, K.; Suzuki, S.; Fuyuhito, A.; Yamamoto, K.; Sato, K.; Shiomi, D.; Naito, A.; Takui, T.; Nakasuji, K. *Angew. Chem., Int. Ed.* **2002**, *41*, 1793.
(5) (a) Dutta, P.; Maiti, S. K.; Karmakar, S. N. *Org. Electron.* **2010**, *11*, 1120. (b) Chang, Y. C.; Chao, I. *J. Phys. Chem. Lett.* **2010**, *1*, 116. (c) Yang, W. B.; Wan, X. J.; Chem., Y. S. *J. Mol. Struct.* **2010**, *968*, 85. (d) Fan, Z. Q.; Chen, K. Q. *Appl. Phys. Lett.* **2010**, *96*, 053509. (e) Yang, W. B.; Wang, X. J.; Xu, Y. F.; Lv, X.; Chen, Y. S. *Synth. Met.* **2009**, *159*, 17.
(6) (a) Zaitsev, V.; Rosokha, S. V.; Head-Gordon, M.; Kochi, K. *J. Org. Chem.* **2006**, *71*, 520. (b) Small, D.; Rosokha, S. V.; Kochi, J. K.; Head-Cordon, M. *J. Phys. Chem. A* **2005**, *109*, 11261. (c) Small, D.; Zaitsev, V.; Jung, Y. S.; Rosokha, S. V.; Head-Gordon, M.; Kochi, J. K. *J. Am. Chem. Soc.* **2004**, *126*, 13850.
(7) (a) Ukai, T.; Nakata, K.; Yamannaka, S.; Kubo, T.; Morita, Y.; Takada, T.; Yamaguchi, K. *Polyhedron* **2007**, *26*, 2313. (b) Takano, Y.; Taniguchi, T.; Isobe, H.; Kubo, T.; Morita, Y.; Yamamoto, K.; Nakasuji, K.; Takui, T.; Yamaguchi, K. *J. Am. Chem. Soc.* **2002**, *124*, 11122. (c) Takano, T.; Taniguchi, T.; Isobe, H.; Kubo, T.; Morita, Y.; Yamamoto, K.; Nakasuji, K.; Takui, T.; Yamaguchi, K. *Chem. Phys. Lett.* **2002**, *358*, 17.
(8) (a) Tian, Y.; Kertesz, M. *J. Am. Chem. Soc.* **2010**, *132*, 10648. (b) Tian, Y.-H.; Huang, J.; Kertesz, M. *Phys. Chem. Chem. Phys.* **2010**, *12*, 5084. (c) Huang, J.; Kertesz, M. *J. Phys. Chem. A* **2007**, *111*, 6304. (d) Huang, J.; Kertesz, M. *J. Am. Chem. Soc.* **2007**, *129*, 1634. (e) Huang, J.; Kertesz, M. *J. Am. Chem. Soc.* **2006**, *128*, 1418. (f) Huang, J.; Kertesz, M. *J. Am. Chem. Soc.* **2006**, *128*, 7277.
(9) Craciun, S.; Donald, K. J. *Inorg. Chem.* **2009**, *48*, 5810.
(10) Mota, F.; Miller, J. S.; Novoa, J. J. *J. Am. Chem. Soc.* **2009**, *131*, 7699.

 Published on Web 12/06/2010

Chart 1. Phenalenyl Radical (1) and Its SOMO

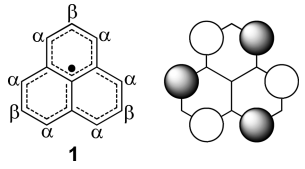

Scheme 1. σ-Dimerization of Phenalenyl and π-Dimerization of 2,5,8-Tri-*tert*-butylphenalenyl

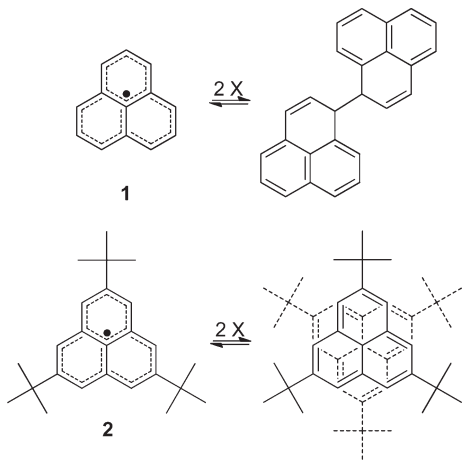

derivatives to form π-dimers in addition to σ-dimers. The π-dimerization is illustrated with a β-substituted tri-*tert*-butylphenalenyl radical (**2**, Scheme 1), where the bulky *tert*-butyl groups prevent the σ-dimerization. X-ray diffraction shows that **2** forms staggered π-dimers with an average intermolecular separation of 3.306 Å between the six pairs of eclipsed spin-bearing α-C atoms on the periphery (cf. the SOMO in chart 1).[12] Other experiments using ESR, UV−vis, and MS also confirm the π-dimerization of **2** in solutions[6c] and even in the gas phase.[13]

Although the understanding of the σ-dimerization is straightforward, the nature of the π-dimerization is theoretically challenging. Simply on the basis of the intermolecular separation that is shorter than the sum of the van der Waals (vdW) radii, it can be anticipated that there should exist an additional force to bring the two radicals slightly closer than the vdW distance. From a molecular orbital theory argument, the overlap of two SOMOs of π-stacked phenalenyls can lead to a bonding dimer orbital. After a number of intensive experimental and theoretical efforts during the past decade, the intermolecular interactions associated with the π-dimerization have now been recognized as a new class of two-electron/multicenter (2e/mc) $\pi-\pi$ bonding interaction.[6−8,10−13] Depending on the radical molecules forming the π-dimer or the packing offset of one molecule with respect to the other, the number of centers in 2e/mc can be different.[7b,14] For **2**, this is a 2e/12c bonding since the six pairs of eclipsed spin-bearing C atoms participate in the SOMO−SOMO overlap. Note that as an alternative based on an AIM study of the bond-critical points, Mota et al. argue that the π-dimer of **2** has a dominant 2e/14c bonding character (including the eclipsed pair of C atoms in the center).[10]

One prominent characteristic of the 2e/mc bonding of phenalenyl π-dimers is the similar strength of $\pi-\pi$ bonding compared to σ-bond formation. The binding energy for the staggered π-dimer of **2** is −9.5 and −8.8 kcal/mol in CH_2Cl_2 solution according to ESR and UV−vis spectral measurements, respectively.[6c] On the other hand, the binding energy for the σ-dimer of **1** is only −9.8 (±0.7), −10 (±1), and −11.34 (±0.11) kcal/mol in toluene,[2] CH_2Cl_2,[6a,b] and CCl_4 solutions,[2] respectively, which appear to be small compared to regular C−C σ-bond energies. This is probably because of the crowdedness of the dimer and the high stability of the monomer. Toluene tends to decrease the binding energy through the $\pi-\pi$ interactions with **1**, which favors the dissociation of the σ-dimers.[2] Because of the similarity between the solvents of CH_2Cl_2 and CCl_4, it is possible to compare the binding energy for the π-dimer of **2** with that for the σ-dimer of **1** in these solvents. Further joint experimental and theoretical studies[6a,b] on different phenalenyl derivatives, together with the values shown above, indicate that the 2e/mc $\pi-\pi$ bonding of phenalenyl π-dimers is close in energy to the σ-bond of phenalenyl σ-dimers and the energetic preference for σ-dimerization over π-dimerization is only 1−5 kcal/mol.

Potential applications of phenalenyl-based molecular materials are closely associated with the breaking/making of the multicenter $\pi-\pi$ bonding versus the various possible σ-bonds that can connect the two phenalenyl units. The breaking/making of bonds may take place independently or manifest as the valence tautomerization between the two bonding motifs. The variations of physicochemical properties of phenalenyl derivatives are enabled by such bond fluctuations, giving rise to "smart" π-functional materials that are sensitive to and react to environmental stimuli. For example, Itkis et al. found that ethyl- and butyl-substituted spiro-biphenalenyls form π-dimers that exhibit temperature-dependent bistabilities in three physical channels: magnetism, conductivity, and infrared absorption.[11b] It is noteworthy that the phase transitions and concomitant property changes of these materials are either below or above room temperature depending on substituents, showing the potential of room-temperature applications. Morita et al. found that the reversible thermochromism of a diazaphenalenyl can be ascribed to the tautomerization between σ- and π-dimers.[11c]

(11) (a) Pal, S. K.; Itkis, M. E.; Tham, F. S.; Reed, R. W.; Oakley, R. T.; Haddon, R. C. *Science* **2005**, *309*, 281. (b) Itkis, M. E.; Chi, X.; Cordes, A. W.; Haddon, R. C. *Science* **2002**, *296*, 1443. (c) Morita, Y.; Suzuki, S.; Fukui, K.; Nakazawa, S.; Kitagawa, H.; Kishida, H.; Okamoto, H.; Naito, A.; Sekine, A.; Ohashi, Y.; Shiro, M.; Sasaki, K.; Shiomi, D.; Sato, K.; Takui, T.; Nakasuji, K. *Nat. Mater.* **2008**, *7*, 48. (d) Phenalenyl-based molecular materials also display substantial nonlinear optical (NLO) responses, owing to their intermediate biradicaloid character. See for example: Nakao, M.; Kishi, R.; Ohta, S.; Takahashi, H.; Kubo, T.; Kamada, K.; Ohta, K.; Botek, E.; Champagne, B. *Phys. Rev. Lett.* **2007**, *99*, 033001.

(12) (a) Goto, K.; Kubo, T.; Yamamoto, K.; Nakasuji, K.; Sato, K.; Shiomi, D.; Takui, T.; Kubota, M.; Kobayashi, T.; Yakusi, K.; Ouyang, J. Y. *J. Am. Chem. Soc.* **1999**, *121*, 1619. (b) Fukui, K.; Sato, K.; Shiomi, D.; Takui, T.; Itoh, K.; Goto, K.; Kubo, T.; Yamamoto, K.; Nakasuji, K.; Naito, A. *Synth. Met.* **1999**, *103*, 2257.

(13) Suzuki, S.; Morita, Y.; Fukui, K.; Sato, K.; Shiomi, D.; Takui, T.; Nakasuji, K. *J. Am. Chem. Soc.* **2006**, *128*, 2530.

(14) Miller, J. S.; Novoa, J. J. *Acc. Chem. Res.* **2007**, *40*, 189.

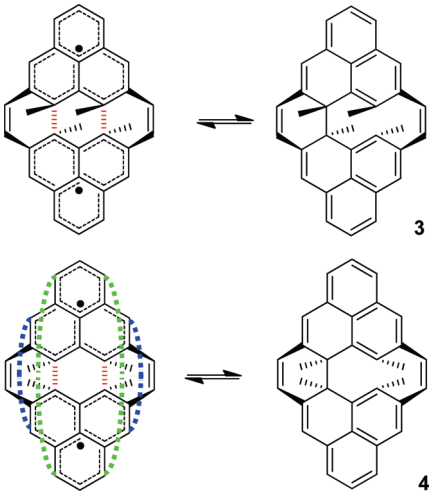

Figure 1. Valence tautomerizations between π-dimers (left column) and σ-dimers (right column) of the chair (**3**) and boat conformations (**4**) of cyclo-biphenalenyl biradicaloid molecule. The nomenclature of chair and boat conformations follows cyclohexane due to the similarities to the latter at the central six-membered rings for the π-dimers. The red/green/blue dashed lines/curves indicate the 2e/mc $\pi-\pi$ bondings. For clarity, the hydrogen atoms are not shown.

In this work, our interest in phenalenyl-based molecular materials is motivated by the applications of phenalenyl derivatives as π-functional materials on the basis of valence tautomerization between σ- and π-dimers of phenalenyl derivatives. Specifically, we examine two cyclo-biphenalenyl biradicaloid molecular materials with chair (**3**) and boat conformations (**4**) as shown in Figure 1 using density functional theory (DFT). In these molecules, the two phenalenyl radical units are connected by two "clamps" made up of etheno-units. These clamps hold the two SOMO-like subunits in each other's vicinity and therefore create an environment where both σ- and π-bonding remain competitive leading to the fluxional structure that is at the center of this study. Because of the analogy to phenalenyl dimers, we will refer to these interactions as σ- and π-dimerization although these interactions in this case refer to intramolecular interactions. The choice of DFT was first validated by comparing the theoretical geometries and energetics with the available experimental results for the chair conformation.[15] The 2e/mc bonding characteristics of the π-dimers, tautomerizations, and magnetic properties of both the chair and boat conformations were studied using the validated DFT. Thermochromism properties were predicted based on the absorption spectra calculations.

2. Computational Methodologies

For the two biradicaloid molecular materials, we performed molecular instead of solid-state calculations for the following two reasons: (1) the chair conformation has been shown to be a molecule-based material and neighboring molecules in the condensed phase are well separated by the vdW distance;[15] (2) it is expected that, if the boat conformation is synthesized, the intermolecular interactions will be weaker than the intramolecular forces and thus the latter will prevail over the former, making the conformation investigation essentially a molecular problem. As noted in our previous work, the tautomerizations between σ- and π-dimers cause the electron conjugations to change drastically.[8b,f] A multireference-based description with all of the active electrons included would be desirable but the computational cost is prohibitively high. Herein, we will resort to DFT for geometry optimizations and energy/frequency calculations. We will show that the selected DFT is able to produce quantitative results along the tautomerization pathway.

On the Jacob's ladder of DFT, Perdew and Schmidt envision five rungs of functionals with increasing degree of precision (and also computational cost) varying from the earliest local density approximation (LDA), generalized gradient approximations (GGAs), meta-GGAs, hybrid functionals, and to fully nonlocal functionals.[16] For our studies, the M06-class meta-GGAs recently developed by Zhao and Truhlar[17] are employed, with occasional comparison to the most widely used Becke's three-parameter hybrid functional in combination with Lee−Yang−Parr correlation functional (B3LYP).[18] In spite of its popularity, B3LYP has been recognized to systematically underestimate reaction barrier heights.[17,19] M06-class of meta-GGAs, which contain the explicit dependence on kinetic energy density, were developed to better address the reaction barrier heights and dispersion interactions. Depending on the amount of Hartree−Fock (HF) exchange, there are four M06 functionals to choose from: M06-L (HF exchange =0%), M06 (27%), M06−2X (54%), M06-HF (100%). Our experience using an earlier version of M06-class functionals, i.e. M05−2X, shows that such meta-GGA is suitable for the investigations of the fluxional σ-bonds of diazaphenalenyl dimers.[8b]

The potential energy surface (PES) of the two conformations of cyclo-biphenalenyls was explored by performing geometry optimizations for the σ- and π-dimers, and by a transition state (TS) search on the PES. Both the spin-restricted (R) method and the broken-symmetry (BS) method within the spin-unrestricted (U) scheme were used. The BS approach is not available in the standard version of the NWChem program used for PES studies and therefore it was added for this work. Specifically, the HOMO and LUMO are mixed to lift the spatial symmetries, thus producing spin-unrestricted wave functions for the initial guess for the singlet states. For the σ-dimers and the transition states, the singlet ground states are investigated. We found that restricted and unrestricted theories produce the same results for these structures, indicating that their electronic structures are closed-shell and there are no BS solutions for these structures (in other words, if BS approach were forced on these structures, the wave functions would be exactly the same as those obtained using restricted theory). For the π-dimers, their ground states could be closed-shell or open-shell singlet states but there also exist low-lying excited triplet states. The geometries of the closed-shell singlets (R) and the open-shell singlets (U) are optimized using the restricted and unrestricted theories, respectively. Depending on theories and the amount of HF exchange, restricted DFT could be unstable with respect to the unrestricted method and therefore R- and U- solutions will be different (in such cases, different levels of theory will be prefixed with either

(15) Rohrbach, W. D.; Boekelheide, V.; Hanson, A. W. *Tetrahedron Lett*. **1985**, *26*, 815.
(16) Perdew, J. P.; Schmidt, K. In *Density Functional Theory and Its Applications to Materials*; Van Doren, V. E., Van Alsenoy C., Geerlings, P., Eds.; AIP Conference Proceedings; American Institute of Physics: Melville, NY, 2001; Vol. *577*, pp 1−20.
(17) Zhao, Y.; Truhlar, D. G. *Acc. Chem. Res*. **2008**, *41*, 157.
(18) (a) Becke, A. D. *J. Chem. Phys*. **1993**, *98*, 5648. (b) Lee, C.; Yang, W.; Parr, R. G. *Phys. Rev. B* **1998**, *37*, 785.
(19) Sousa, S. F.; Fernandes, P. A.; Ramos, M. J. *J. Phys. Chem. A* **2007**, *111*, 10439.

R or U). The lower energies of unrestricted DFTs are related to the slightly weaker $\pi-\pi$ bonding compared to σ-bond as a result of static (or nondynamical) electron correlation.[20] Low-lying triplet energies of the π-dimers were obtained from single-point energy calculations using the open-shell singlet π-dimer structures optimized by unrestricted DFT. These energies are used for magnetic susceptibility calculations of both chair and boat conformations. Pople's 6-31G* basis set was used for all DFT calculations. We have verified using other phenalenyl-derivatives that a larger basis set, 6-311+G(2d), does not modify the conclusions obtained with 6-31G*.[8d,f] Vibrational analysis was performed for key stationary points to verify their identities as minima or transition states and to obtain thermochemical data used for zero-point energy corrections and for calculations of enthalpies or Gibbs free energies.

The NWChem suite of programs[21] was used for the explorations of PES. The Gaussian 03 suite of programs[22] was employed to calculate nucleus-independent chemical shifts (NICSs),[23] which are used to evaluate the aromaticity of the π-dimers. Mayer bond orders (MBOs)[24] offer a general guide to characterize covalent interactions and herein are used to depict the $\pi-\pi$ bondings. MBOs at the overlapping C pairs were calculated for σ-, π-dimers, and transition states using the NBO 5.0 program.[25] In order to predict the thermochromism of both molecular materials, the UV−vis spectroscopies of σ- and π-dimers were calculated using Gaussian 03[22] at the level of the parametrized ZINDO/S method.[26] Singly excited configuration interaction (CI) calculations were performed with eight occupied and eight virtual orbitals included. To provide a unified DFT interpretation, we also performed time-dependent density functional theory (TDDFT)[27] calculations at the M06/6-31G* level using the Gaussian 09 programs.[28] To reduce computational cost, inner shells are excluded from the correlation calculations.

3. Results and Discussion

In this section, we first validate the selection of DFT using the experimental results of the chair conformation **3**. We then apply the validated DFT to the PES and magnetism of **3** and **4**. In the next step, the stacked $\pi-\pi$ bonding of the π-dimers of **3** and **4** are characterized by bond order calculations, and the concomitant aromaticities are probed with the aid of NICS indices. Finally, thermochromism properties are discussed.

Scheme 2. [3,3]-Sigmatropic (Cope) Rearrangement of the Chair Conformation 3 (note the highlighted 1,5-hexadiene fragment in the center of 3 or 3′, and the $\pi-\pi$ overlap in 5)

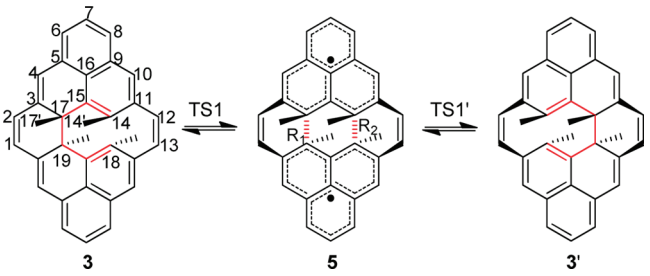

Scheme 3. Cope Rearrangement of 1,5-Hexadiene (6)

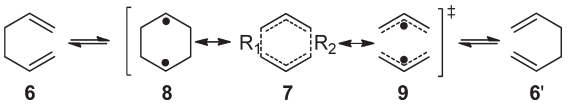

Validation of Theories with 3. The chair conformation **3** was synthesized and characterized by X-ray diffraction more than two decades ago.[15] The X-ray structure of **3** exhibits a 4-fold disorder, coming from the enantiomeric mixture of rearrangement products and the different orientations of them. As can be seen from Scheme 2, the [3,3]-sigmatropic rearrangement reaction leads to the back-and-forth shift of the σ-bond that connects the two phenalenyl units. The rearrangement kinetics of **3** was studied using variable temperature (dynamic) NMR.[15] From the highlighted central fragment of **3** and its enantiomer **3′**, this rearrangement resembles the extensively studied archetypical Cope rearrangement of 1,5-hexadiene (**6**, Scheme 3).[29,30] However, the significance of the rearrangement mechanism of **3** was not appreciated by theoretical investigators until the rearrangement was found to have a stepwise mechanism proceeding through a C_{2h} π-dimerized intermediate **5** with a very long interphenalenyl distance R ($R_1 = R_2 \approx 2.8$ Å).[8f] In sharp contrast, the rearrangement of **6** has a concerted mechanism proceeding via an aromatic chairlike C_{2h} transition state **7**, which has an interallylic bond length of $R \approx 2.0$ Å.[31] Substitutions that stabilize cyclohexane-1,4-diyl (**8**) that has a relatively short R and/or bis-allyl diradical (**9**) that has a relatively long R may enhance the contributions from these resonance structures, leading to a rather large R range from 1.7 to 2.6 Å.[32] Theoretical studies found some exceptions

(20) Parkhill, J. A.; Head-Gordon, M. *J. Chem. Phys.* **2010**, *133*, 024103.
(21) Bylaska, E. J.; de Jong, W. A.; Govind, N.; Kowalski, K.; Straatsma, T. P.; Valiev, M.; Wang, D.; Apra, E.; Windus, T. L.; Hammond, J. et al. *NWChem, A Computational Chemistry Package for Parallel Computers, Version 5.1*; Pacific Northwest Laboratory: Richland, WA, 2007
(22) Frisch, M. J.; Trucks, G. W.; Schlegel, H. B.; Scuseria, G. E.; Robb, M. A.; Cheeseman, J. R.; Montgomery, J. A., Jr.; Vreven, T.; Kudin, K. N.; Buran, J. C.; et al.; *Gaussian 03, Revision D.01*; Gaussian, Inc.: Wallingford, CT, 2004.
(23) Chen, Z.; Wannere, C. S.; Corminboeuf, C.; Puchta, R.; Schleyer, P. v. R. *Chem. Rev.* **2005**, *105*, 3842.
(24) Mayer, I. *Chem. Phys. Lett.* **1983**, *97*, 270.
(25) Glendening, E. D.; Badenhoop, J, K.; Reed, A. E.; Carpenter, J. E.; Bohmann, J. A.; Morales, C. M.; Weinhold, F. *NBO 5.0*; Theoretical Chemistry Institute, University of Wisconsin, Madison, WI, 2001.
(26) (a) Bacon, A. D.; Zerner, M. C. *Theor. Chim. Acta* **1979**, *53*, 21. (b) Ridley, J. E.; Zerner, M. C. *Theor. Chim. Acta* **1976**, *42*, 223.
(27) (a) Bauernschmitt, R.; Ahlrichs, R. *Chem. Phys. Lett.* **1996**, *256*, 454. (b) Casida, M. E.; Jamorski, C.; Casida, K. C.; Salahub, D. R. *J. Chem. Phys.* **1998**, *108*, 4439. (c) Stratmann, R. E.; Scuseria, G. E.; Frisch, M. J. *J. Chem. Phys.* **1998**, *109*, 8218–24.
(28) Frisch, M. J.; Trucks, G. W.; Schlegel, H. B.; Scuseria, G. E.; Robb, M. A.; Cheeseman, J. R.; Scalmani, G.; Barone, V.; Mennucci, B.; Petersson, G. A. et al. *Gaussian 09, Revision A.02*; Gaussian, Inc.: Wallingford CT, 2009.
(29) Gajewski, J. J. *Hydrocarbon Thermal Isomerizations*; Academic Press: New York, 1981; pp 166−76.
(30) (a) Staroverov, V. N.; Davidson, E. R. *J. Am. Chem. Soc.* **2000**, *122*, 186. (b) Kozlowski, P. M.; Dupius, M.; Davidson, E. R. *J. Am. Chem. Soc.* **1995**, *117*, 774. (c) Jiao, H.; Schleyer, P. v. R. *Angew. Chem., Int. Ed.* **1995**, *34*, 334. (d) Hrovat, D. A.; Morokuma, K.; Borden, W. T. *J. Am. Chem. Soc.* **1994**, *116*, 1072. (e) Wiest, O.; Black, K. A.; Houk, K. N. *J. Am. Chem. Soc.* **1994**, *116*, 10336. (f) Dewar, M. J. S.; Jie, C. *Acc. Chem. Res.* **1992**, *25*, 537.
(31) (a) Staroverov, V. N.; Davidson, E. R. *J. Mol. Struct. (THEOCHEM)* **2001**, *573*, 81.(b) Wiest, O. In *Encyclopedia of Computational Chemistry*; Schleyer, P. v. R., Ed.; Wiley: Chichester, U.K., 1998; Vol. *5*, p 3111. (c) Borden, W. T.; Davidson, E. R. *Acc. Chem. Res.* **1996**, *29*, 67. (d) Houk, K. N.; Gonzalez, J.; Li, Y. *Acc. Chem. Res.* **1995**, *28*, 81.
(32) Doering, W. v. E.; Wang, Y. *J. Am. Chem. Soc.* **1999**, *121*, 10112.

Table 1. Calculated Geometries of the σ-Dimer of the Chair Conformation 3 Using the M06-class of Meta-GGA Functionals and B3LYP Hybrid Functional Compared with the Experimental Result from X-ray Diffraction

bond index[a]	M06-L[b,c]	M06[b,c]	M06-2X[b,c]	M06-HF[b,c]	B3LYP[c,d]	exp.[e]
HF exchange (%)	0	27	54	100	20	
C1−C2	1.355	1.349	1.344	1.339	1.354	1.32
C2−C3	1.447	1.455	1.465	1.479	1.460	1.47
C3−C4	1.353	1.346	1.343	1.336	1.352	1.36
C3−C17	1.522	1.521	1.525	1.525	1.529	1.56, 1.51
C4−C5	1.434	1.441	1.450	1.462	1.446	1.43
C5−C6	1.390	1.384	1.382	1.375	1.390	1.39
C5−C16	1.430	1.428	1.430	1.430	1.434	1.42
C6−C7	1.402	1.404	1.408	1.413	1.407	1.38
C7−C8	1.377	1.374	1.372	1.368	1.379	1.36
C8−C9	1.415	1.414	1.418	1.421	1.419	1.38
C9−C10	1.411	1.412	1.416	1.421	1.418	1.42
C9−C16	1.429	1.424	1.421	1.414	1.431	1.43
C10−C11	1.378	1.373	1.371	1.366	1.378	1.36
C11−C12	1.472	1.477	1.485	1.495	1.484	1.47
C11−C14	1.439	1.438	1.441	1.445	1.444	1.48, 1.43
C12−C13	1.354	1.350	1.347	1.343	1.355	1.32
C14−C14′	1.506	1.508	1.516	1.525	1.519	1.45, 1.47
C14−C15	1.406	1.401	1.397	1.390	1.406	1.43, 1.46
C15−C16	1.433	1.433	1.438	1.443	1.438	1.44
C15−C17	1.526	1.527	1.531	1.532	1.535	1.48, 1.50
C17−C17′	1.547	1.547	1.552	1.557	1.561	1.61, 1.62
C17−C19 (R_1)	1.670	1.658	1.657	1.643	1.685	1.63
C14−C18 (R_2)	2.668	2.664	2.675	2.633	2.686	2.65
rms deviation[f]	0.0209	0.0182	0.0193	0.0205	0.0247	-

[a] Atomic numbering of **3** is shown in Scheme 2. [b] M06-class of meta-GGA functionals; see ref 17. [c] 6-31G* basis set. [d] B3LYP hybrid functional; see ref 18. [e] X-ray diffraction in ref 15. [f] Excluding the bond lengths with two values.

where the Cope rearrangement of substituted **6** can be stepwise going through a diradicaloid intermediate with a rather short R around 1.6 Å.[33] Nevertheless, compared with the transition states **7**-**9**, the intermediate **5** is considered to be unusual[34] as it is stabilized by the 2e/4c $\pi-\pi$ bonding due to the through-space $\pi-\pi$ overlap (Scheme 2). Note that the previous investigations at the B3LYP level should be deemed as semiquantitative, in that the reaction barrier height from the reactant **3** to the intermediate **5** is 4.6 kcal/mol,[8f] while the experimental measurement using dynamic NMR found a larger value of 9 (±1) kcal/mol.[15]

In light of the improvements offered by the M06-class of meta-GGAs, it is necessary to compare the results from the M06-class with those from B3LYP and confront them with available experimental results for this category of molecules. The optimized geometries for the reactant **3** at various levels of theory are tabulated in Table 1, along with the X-ray structure of **3**. Examining the B3LYP column first, we found that due to the 4-fold disorder observed in the X-ray structure, the agreement between calculations and experiments cannot be claimed to be excellent although it is expected to be so based on the track record of B3LYP for molecular geometry optimizations. Although about half of the bonds have a discrepancy less than 2 pm between theory and experiment, very large disparities stand out for bonds involving atoms C14 and C17, e.g. C14−C14′ and C17−C17′. The experimental 1.61 or 1.62 Å for C17−C17′ is probably too long for a C−C bond between two sp^3-hybridized C atoms, and the experimental 1.45 or 1.47 Å for C14−C14′ seems to be too short for a bond between sp^2- and sp^3-hybridized C atoms.[35] Due to the 4-fold disorder, the X-ray data may not correctly represent the individual bond length, as pointed out by experimentalists.[15] It is therefore expected that X-ray measurements at lowered temperatures would be able to produce a more reliable structure to be compared with DFT results. Comparing the optimized geometries across the M06-class meta-GGAs with that of B3LYP, we found that all of the meta-GGAs produced slightly better geometries in terms of smaller root-mean-square (rms) deviations than B3LYP. In addition, M06 appears to be the best among the meta-GGAs used. We shall see in the following that this level of theory is also the best for reaction barrier heights.

Next, we optimized the geometries of the π-dimer **5** (Scheme 2) with both the M06-class and B3LYP functionals using restricted and unrestricted theories (the atomic coordinates are provided in Supporting Information). The RB3LYP and UB3LYP results obtained using NWChem are virtually the same as those reported earlier.[8f] Because the BS approach was newly programmed into NWChem, this ensures the reliability of using the BS approach for meta-GGA functionals. We found that for DFT functionals with HF exchange less than 30% (including M06-L, M06, and B3LYP), there are two solutions (R and U) for the π-dimer geometry. The interphenalenyl distances are R = 2.798 (2.865), 2.768 (2.977), 2.818 (3.042) Å

(33) (a) Navarro-Vázquez, A.; Prall, M.; Schreiner, P. R. *Org. Lett.* **2004**, *6*, 2981. (b) Hrovat, D. A.; Chen, J.; Houk, K. N.; Borden, W. T. *J. Am. Chem. Soc.* **2000**, *122*, 7456. (c) Hrovat, D. A.; Beno, B. R.; Lange, H.; Yoo, H.-Y.; Houk, K. N.; Borden, W. T. *J. Am. Chem. Soc.* **1999**, *121*, 10529.

(34) (a) Bachrach, S. M. *Annu. Rep. Prog. Chem., Sect. B* **2008**, *104*, 394. (b) Armstrong S. K. Molecular rearrangements: part 1. pericyclic reactions. In *Organic Reaction Mechanism*; Knipe, C., Ed.; John Wiley & Sons: New York, **2010**; pp 419−450. (c) Wang Z. Cope Rearrangement. In *Comprehensive Organic Name Reactions and Reagents*; John Wiley & Sons: Hoboken, NJ, **2009**; pp 702−708.

(35) Pople, J. A.; Gordon, M. *J. Am. Chem. Soc.* **1967**, *89*, 4253.

Table 2. Cope Rearrangement Energetics and Barrier Heights of 3 between the Transition State and the σ-Dimer Calculated with the M06-class of Meta-GGA Functionals and B3LYP Hybrid Functional Compared with the Experimental Result from the Dynamic NMR Experiment

	M06-L[a,b,c]	M06[a,b,c]	M06-2X[a,b,d]	M06-HF[a,b,d]	B3LYP[b,c,e]	Exp.[f]
HF exchange (%)	0	27	54	100	20	
			$\Delta E(\sigma-\pi)$[g]			
R-DFT	−1.4[h]	7.9	13.1	15.1	3.5	
U-DFT	−1.8[h]	3.2	13.1	15.1	1.1	
			Reaction Barrier Heights[i]			
ΔE^0	5.1	9.7	13.1	15.1	6.3	
ΔE^0(ZPE[j])	4.1	8.8	11.3	13.5	5.1[k]	
$\Delta H^{298.15}$	4.1	8.9	12.0	13.6	5.1[k]	
$\Delta G^{298.15}$	4.2	8.3	9.7	13.0	4.6[k]	9 (±1)[l]

[a] M06-class of meta-GGA functionals; see ref 17. [b] 6-31G* basis set. [c] Stepwise mechanism. [d] Concerted mechanism. [e] B3LYP hybrid functional; see ref 18. [f] Variable temperature NMR in ref 15. [g] Energies of π-dimer relative to the σ-dimer, i.e., $E^0(\pi)-E^0(\sigma)$. [h] Cope rearrangement is not practical because the π-dimer is lower in energy than the σ-dimer. [i] The energy of the transition state relative to the σ-dimer. [j] With zero-point energy correction. [k] See ref 8f. [l] The experimental value is most likely obtained based on a concerted reaction mechanism and the value for a stepwise mechanism should be corrected as discussed in the text.

for M06-L, M06, and B3LYP, respectively, where the numbers in parentheses are the BS results. The total spin angular momentum $\langle S^2\rangle$ at the unrestricted level of theory ranges from 0.433, 0.960, to 0.850, respectively, showing the same trend as the amount of HF exchange. For the B3LYP result with the intermediate $\langle S^2\rangle$, we calculated the natural orbital occupation number (NOON) for the LUMO[36] and found a significant singlet biradical character of 50%. However, for DFTs functionals with more than 30% HF exchange, which is the case for M06-2X and M06-HF, restricted and unrestricted theories produce the same results. Frequency calculation reveals that the π-dimer structure with M06-HF is in fact a transition state and therefore the rearrangement has a concerted mechanism, in contrast with the stepwise mechanism with other functionals. The interphenalenyl distances for M06-2X and M06-HF are much shorter at 2.470 and 2.222 Å, respectively. We note that there is no direct way to validate theories for the π-dimer **5**, because it is only theoretically found, but not experimentally observed. Earlier theoretical studies with M05-2X for the staggered π-dimer of **2** (Scheme 1) produced a set of interphenalenyl separations that are close to the experimental values,[8b] providing an indirect evidence that this type of meta-GGA is suitable for the structural studies of phenalenyl π-dimers.

The energies of the π-dimers relative to those of the corresponding σ-dimers are tabulated in Table 2. For M06-L functional, both the restricted and unrestricted energies for the π-dimers are lower than that of the σ-dimer, indicating that the π-dimer is the global minimum. This contradicts the X-ray results and therefore it can be concluded that M06-L is not appropriate for the PES studies of this Cope rearrangement. The M06-2X and M06-HF functionals can also be ruled out because they predict a concerted reaction mechanism (see the transition state search in the following discussion). However, the reaction should go through an intermediate according to the fact that the crystal of **3** has a yellow-orange color[15] and our electronic spectra calculations indicate that the color comes from the π-dimer (see the UV−vis section). In addition, M06-2X and M06-HF produced σ−π energy differences of over 13 kcal/mol. The σ−π energy differences of about a few kcal/mol by M06 and B3LYP appear to agree better with the results from joint experimental and theoretical studies[6a,b] on various other phenalenyl derivatives showing that the 2e/mc π−π-bonded phenalenyl π-dimers are close in energy to the σ-dimers.

To calculate the reaction barrier heights, we also searched for the transition state that connects σ-dimer **3** to π-dimer **5** (Scheme 2). All of the structures and their thermochemical data are provided in the Supporting Information. Once again, the B3LYP results are virtually the same as those reported earlier, with R_1 = 2.231 Å and R_2 = 2.711 Å. With M06-L functional, we found a transition state with R_1 = 2.145 Å and R_2 = 2.688 Å, where the two values differ by 0.543 Å. In comparison, the M06 solution has R_1 = 2.308 Å and R_2 = 2.688 Å, with a smaller difference in bond length. By checking the energies of **3** and **5** at these latter two levels of theory, we found that the energy of **3** is higher than that of **5** with M06-L, whereas it is the opposite with M06. Therefore, the observation that the transition state with M06-L is closer to the σ-dimer while that with M06 is closer to the π-dimer is in line with Hammond's postulate.[37] The pyramidalization angles for C14 or C17 atoms may be used as another option for reaction coordinates,[38] but here we stick to the more convenient R_1 and R_2 distances. With M06-2X, the transition state has an R_1 = 2.463 Å and an R_2 = 2.470 Å, which are very close to the R = 2.470 Å of the π-dimer structure. In fact, the energies and the ZPE corrections between the two structures are virtually the same (see the Supporting Information). However, this maximum of energy has no imaginary frequency, which may indicate a problem with M06-2X for the transition state of this specific rearrangement.

The reaction barrier heights for the Cope rearrangement of **3** are calculated as the energy difference between the transition state and the σ-dimer. The values at various levels of theory are compared in Table 2. We have presented four values for each theory, in terms of total

(36) Jung, Y.; Head-Gordon, M. *ChemPhysChem* **2003**, *4*, 522.

(37) (a) Hammond, G. S. *J. Am. Chem. Soc.* **1955**, *77*, 334–338. (b) Solomons, T. W. G.; Fryhle, C. B. *Organic Chemistry*, 9th ed.; John Wiley & Sons, 2007.

(38) Haddon, R. C.; Chow, S.-Y. *J. Am. Chem. Soc.* **1998**, *120*, 10494.

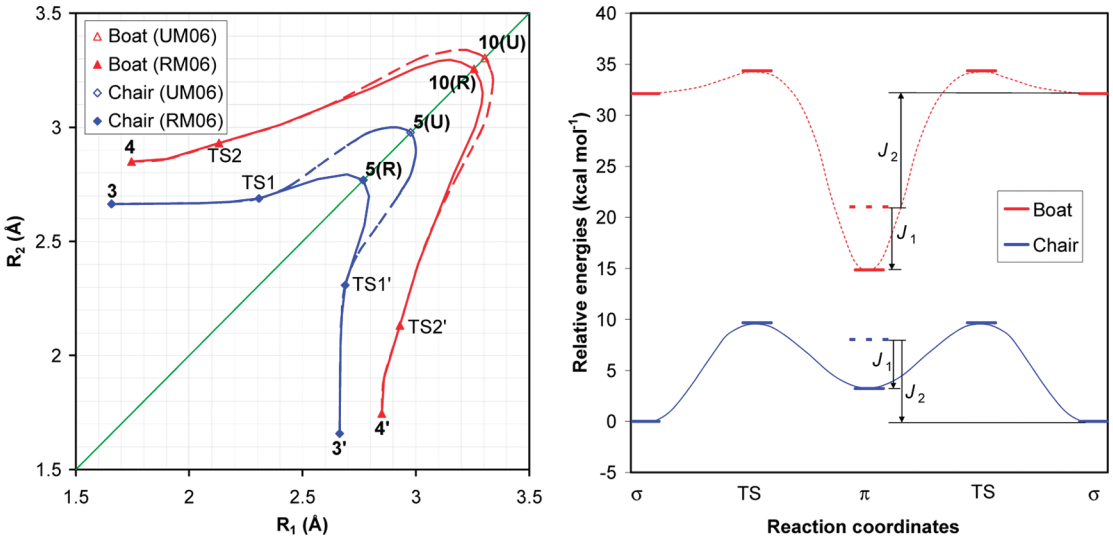

Figure 2. Potential energy surfaces of the chair (**3**) and boat conformations (**4**) of the cyclo-biphenalenyls calculated using R(U)M06/6-31G* in terms of interphenalenyl distances R_1 and R_2 (left panel) (cf. Schemes 2 and 4, respectively) and in terms of total DFT energies relative to that of the σ-dimer of **3** (right panel). Stationary points are discussed in the text. For the right panel, only the π-dimer structures optimized with UM06/6-31G* (BS solutions) are shown, together with their single-point triplet energies at the UM06 geometries. Parameters J_1 and J_2 indicate the energies of the singlet π- and σ-dimers relative to the triplet π-dimers which are used for the paramagnetic susceptibility calculations. The geometries of the stationary points for the boat conformation may distort slightly due to the clustering effect of methyl groups (see the Supporting Information).

DFT energy at 0 K, the total energy at 0 K with zero-point energy (ZPE) correction, enthalpy, and Gibbs free energy at room temperature. The ZPE-corrected energies are in general about 1−2 kcal/mol lower than the total electronic energy and are a good estimate of the enthalpy and Gibbs free energy at room temperature. Among the DFT results, the M06-class functionals give $\Delta G^{298.15}$ ranging from 4.2 to 13.0 kcal/mol, depending on the amount of HF exchange, with the lowest value comparable to the B3LYP result. For the experimental value of 9 (±1) kcal/mol, it was most likely obtained on the basis of a concerted process since the stepwise mechanism of **3**′s Cope rearrangement was unknown at the time of the experiment. Therefore, the calculated barriers can be directly compared to the experimental value for M06-2X and M06-HF because of the concerted mechanism at these two levels of theory. For the other three functionals, however, the reaction is a degenerate stepwise process. The rate constant from the reactant to the intermediate is twice as large as the apparent rate constant for the reaction observed by dynamic NMR according to ref 39 and our derived integrated rate laws (see the Supporting Information), and so the activation barrier of 9 (±1) kcal/mol for a concerted process should be corrected for the stepwise mechanism. However, assuming a coalescence temperature T_c at 273 K (the actual T_c was not reported in ref 15), we found that the correction to the reaction barrier height is less than +0.4 kcal/mol. Although both M06 and M06-2X produce acceptable reaction barrier heights, we choose to use M06 for the rest of these studies because of the more accurate structures obtained with M06 and the problem encountered with the transition state with M06-2X as discussed above.

(39) Friebolin, H. *Basic One- and Two-Dimensional NMR Spectroscopy*; Wiley-VCH: Weinheim, Germany, 1998.

Scheme 4. Putative [3,3]-Sigmatropic (Cope) Rearrangement of the Boat Conformation 4

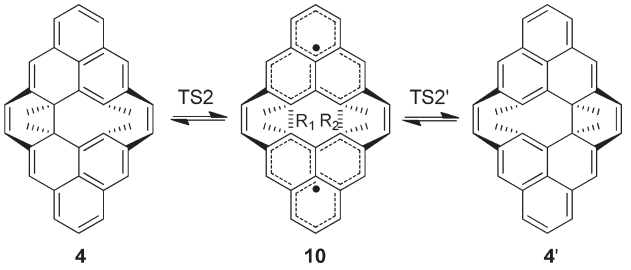

Potential Energy Surfaces. On the basis of the results shown above, in the following we discuss the PES for **3** and **4** using only the M06 functional. As can be seen from the left panel of Figure 2 and Scheme 2, the PES related to the Cope rearrangement of the chair conformation consists of the σ-dimer **3** connected to its enantiomer **3**′ by a π-dimer intermediate **5**, through two symmetrically located transition states TS1 and TS1′. However, depending on the spin restriction, there are two π-dimer structures: the closed-shell singlet by RM06, **5**(R), has an interphenalenyl distance of R = 2.768 Å, whereas the open-shell singlet (i.e., the BS solution) by UM06, **5**(U), has an R = 2.977 Å. The open-shell singlet is 4.7 kcal/mol lower in energy than the closed-shell singlet. On the basis of the understanding for **3**, it is expected that the boat conformation **4** may have a Cope rearrangement as shown in Scheme 4. The PES of **4** is similar to that of its chair counterpart in that **4** is connected to its enantiomer **4**′ by a π-dimer minimum **10**, through symmetrically located transition states TS2 and TS2′. There are also two π-dimer structures, **10**(R) and **10**(U), depending on the spin restriction, but both of them have relative longer interphenalenyl distances at 3.256 and 3.304 Å, respectively. The open-shell singlet is only 0.4 kcal/mol lower in energy than the closed-shell singlet. The energies

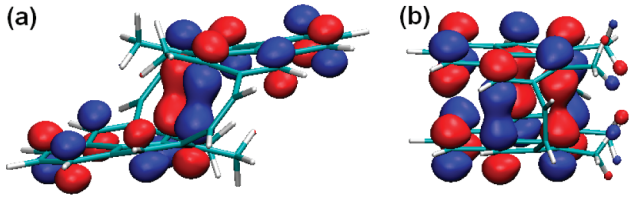

Figure 3. HOMOs of (a) chair and (b) boat conformations showing 2e/4c and 2e/12c $\pi-\pi$ bonding interactions for the π-dimers **5**(R) and **10**(R), respectively.

of σ- and π-dimers for both chair and boat conformations are compared in the right panel of Figure 2. The difference between the chair and boat conformations lies in that the global minimum of the chair conformation is the σ-dimer, whereas it is the π-dimer for the boat conformation. In terms of energy, the π-dimer of the chair is higher than the σ-dimer by only 3.2 kcal/mol. In comparison, the σ-dimer of the boat is higher in energy than the π-dimer by 17.3 kcal/mol. This large energy difference, along with the fact that the global minimum of the boat is a π-dimer, implies that the putative Cope rearrangement described in Scheme 4 does not take place. However, the valence tautomerizations between σ- and π-dimers are still possible at elevated temperatures. We will show that these differences in global minimum structures and energy differences are desirable for potential applications as π-functional materials with different physicochemical properties. In Figure 2 right panel, the low-lying triplet states of the π-dimers are also shown. Parameters J_1 and J_2 indicate the energies of the open-shell singlet π-dimers and closed-shell σ-dimers relative to the triplet π-dimers and their values are used for the paramagnetic susceptibility calculations (see paramagnetism section).

All the similarities and differences presented above are determined by the multicenter $\pi-\pi$ overlap in **5** and **10**. The HOMOs of both **5**(R) and **10**(R) are shown in Figure 3 (for HOMOs of 5(U) and 10(U), see the Supporting Information). For the chair conformation, the four C atoms participating in the tautomerization overlap pairwise, yielding a 2e/4c $\pi-\pi$ bonding. For the boat conformation, however, the two phenalenyl rings are completely eclipsed, thus making a 2e/12c $\pi-\pi$ bonding possible. Studies of various phenalenyl π-dimers with β-substitutions show that the difference of intradimer distances between the slightly shorter α-carbon pairs and the slightly longer central carbon pair increases with increasing bonding strength, which is indicative of stronger attractive forces between the α-carbon pairs due to the SOMO electron pairing.[8a] For **10**, the six pairs of overlapping C atoms have distances of 2×3.256, 2×2.922, and 2×3.485 Å. In spite of the moderately large difference in these overlap distances, the two phenalenyl units are closer to being parallel to each other compared to the "gable" dimer of diazaphenalenyl,[4d] as can be seen from Figure 3b. A phenalenyl π-dimer with eclipsed conformation was discussed theoretically in the context of magnetism,[7b] but only the staggered π-dimer of phenalenyl was observed experimentally.[12] This suggests that experimental work may lead to the observation of this eclipsed dimer that is held together by the two etheno-clamps, not only because the π-dimer **10** is the global minimum but also because it has an average separation of 3.221 Å (or 3.371 Å with UM06) between the peripheral six pairs of eclipsed spin-bearing C atoms, which is comparable to the separation of 3.306 Å for the staggered π-dimer of **2**. For both **5** and **10**, the 2e/mc $\pi-\pi$ bonding stabilizes the dimerized structures, causing them to become minima instead of transition structures.

The $\sigma-\pi$ energy difference is much larger in the case of boat conformation since more C atoms are present in the 2e/12c bonding of **10**, which may strengthen the $\pi-\pi$ bonding. The other reason, which we believe is more important, is that with the boat conformation, the four methyl groups bump pairwise into each other. Methyl groups being too close to each other would increase the energies, especially for the σ-dimer when the σ-bond between two phenalenyl units becomes too short to accommodate methyl groups. As a matter of fact, this bond with $R_1 = 1.746$ Å for the boat is a little longer than that of the chair conformation and other C−C bonds between radical species which is typically around 1.6 Å,[40] showing the effects of intermethyl repulsions. Indeed, by replacing the methyl groups with H atoms, we found that the σ-dimer of the boat conformation becomes lower in energy than the π-dimer by 2.6 kcal/mol. Under such a circumstance, the Cope rearrangement becomes practical. Additional clustering effects of methyl groups, such as the slight geometrical distortion from the symmetrical ones shown in Figure 2 due to the small degree of methyl rotations in the case of **4**, are discussed in the Supporting Information. However, these small distortions do not affect our discussions presented above.

The interphenalenyl distances R_1/R_2 and the corresponding MBOs for the stationary points in Figure 2 are tabulated in Table 3. It can be seen that for both chair and boat conformations, the elongation of R_1 distance from ca. 1.7 Å for the σ-dimer via 2.1−2.3 Å for the transition states to 2.8−3.3 Å for the π-dimers is accompanied by the slight elongation of R_2 distance, with the actual R_1/R_2 values dependent on the conformations and the theories used. Consequently, the MBOs corresponding to R_1 gradually decreases from values close to 1 to values around 0.02−0.11. The MBOs of 0.8−0.9 are reasonable values for stretched σ-bonds. The π-dimer **5**(R) has rather small MBOs for the overlapping C pairs at a value of 0.109. The BS solution **5**(U) has even smaller MBOs with a value of 0.028, which is in agreement with its longer R distances. We note that these non-negligible MBO values, albeit small, are indicative of weak $\pi-\pi$ bonding. This is supported by careful comparisons of the MBOs across the 13 pairs of C atoms in the case of **10**(R) or **10**(U). Among all of these C pairs, only the 6 pairs of spin-bearing α-C atoms have non-negligible MBOs. For **10**(R), the 7 pairs of nonspin-bearing C atoms have negligible MBOs, in the range of 0.001−0.003, while the

(40) (a) 1.599 Å between two spiro-biphenalenyl neutral radicals: Liao, P.; Itkis, M. E.; Oakley, R. T.; Tham, F. S.; Haddon, R. C. *J. Am. Chem. Soc.* **2004**, *126*, 14297. (b) 1.626 Å between two TCNQ anion radicals: Radhakrishnan, T. P.; Van Engen, D.; Soos, Z. G. *Mol. Cryst. Liq. Cryst.* **1987**, *150*, 473. (c) 1.597 Å between two C_{60} anion radicals or 1.584 Å between two C_{70} anion radicals: Konarev, D. V.; Khasanov, S. S.; Saito, G.; Otsuka, A.; Yoshida, Y.; Lyubovskaya, R. N. *J. Am. Chem. Soc.* **2003**, *125*, 10074.

Table 3. Summary of Inter-phenalenyl Distances and Mayer Bond Orders (MBO) for the Stationary Points on the PES of Both Chair (3) and Boat Conformations (4)

structures		C17−C19		C14−C18	
		R_1 (Å)	MBO	R_2 (Å)	MBO
chair[a]	**3** (σ)	1.658	0.868	2.664	0.043
	TS1[b]	2.308	0.341	2.688	0.097
	5(R)/**5**(U) (π)	2.768,[c] 2.977[d]	0.109,[c] 0.028[d]	2.768,[c] 2.977[d]	0.109,[c] 0.028[d]
boat[e]	**4** (σ)	1.746	0.812	2.850	0.023
	TS2[b]	2.132	0.519	2.930	0.041
	10(R)/**10**(U) (π)[f]	3.256,[c] 3.304[d]	0.042,[c] 0.018[d]	3.256,[c] 3.304[d]	0.042,[c] 0.018[d]

[a] For atomic numberings, see Scheme 2. [b] See Figure 2. [c] RM06/6-31G*. [d] UM06/6-31G*. [e] Following the same atomic numbering scheme as the chair. [f] For four other $\pi-\pi$ overlapping pairs, see the discussions in the text.

rest pairs have MBOs of 2×0.042 (in Table 3), 2×0.029, and 2×0.052, giving a sum of 0.246, which can be used to characterize the overall binding qualitatively. This is somewhat larger than the case of chair conformation **5**(R) with a sum of $2 \times 0.109 = 0.218$, which may indicate that the $\pi-\pi$ bonding in **10** is slightly stronger than in **5** and contributes partially to the stabilization of the π-dimer of the boat conformation relative to the σ-dimer (Figure 2). It is noteworthy that the MBOs corresponding to R_2 increases as the stationary points shift on the PES from the σ- to the π-dimers, although the R_2 distances increases marginally as well. This corroborates the existence of $\pi-\pi$ bonding in the π-dimerized intermediates.

We further characterize the aromaticity of the π-dimerized intermediates by computing their NICS values using the RM06 optimized geometries with the B3LYP functional. Usually, NICSs are calculated at 1 Å above the ring centers. In contrast, here we performed the calculations at the center of mass for each six-membered ring because it is much easier to define ghost atoms at these locations.[41] For **5**(R), we obtained −9.88 ppm and two equal values of −5.18 ppm on one phenalenyl unit. The other phenalenyl has the same values by symmetry. For **10**(R), we obtained −8.53 ppm and twice −6.60 ppm on one of two phenalenyl units. These values are comparable to the NICS value of −8.0 ppm at the ring center of benzene molecule.[23] For **10**(R), we also checked the NICS values at locations halfway between overlapping ring centers and obtained −13.42 and twice −14.14 ppm. These strongly negative NICS values are indicative of the aromaticity of the eclipsed phenalenyl π-dimer. Experimental and theoretical work on the staggered π-dimer of **2** found that its π-dimerization is partly stabilized by aromaticity.[13] We note that the aromaticity may originate from the cage-like structure due to the head-over-head $\pi-\pi$ overlap of HOMO orbitals (Figure 3). Returning to **5**(R), the only location to check the cage aromaticity is at the center of the entire molecule, where we obtained a high NICS value of −15.07 ppm. All of the locations for NICS calculations are illustrated in Figure S1 in the Supporting Information.

On the basis of the multicenter $\pi-\pi$ overlap of the two SOMO orbitals shown in Figure 3b and non-negligible MBOs for the six pairs of α-C atoms discussed above, we wondered if the two phenalenyl units in **10** may undergo σ-dimerization reactions at other four α-C pairs in addition to forming **4** and **4′**. This is similar to the dimerization reactions of two diazaphenalenyl radicals as was shown both experimentally[11c] and by theoretical modeling[8b] of its PES. We explored the PES of **4** and found that indeed there are other local minima. As shown in Figure 4, there are one π-dimer (**10**) and six low-lying σ-dimers on the PES (atomic coordinates provided in the Supporting Information). Similar to the degenerate **4** and **4′** that are connected to the π-dimer by two degenerate transition states TS2 and TS2′, respectively, σ-dimers **11** and **12** could dissociate to form the π-dimer **10** via transition states TS3 and TS4. Symmetry allows two more enantiomeric σ-dimer and two more transition states. The presence of these stationary points completes the PES of **4** shown in Figure 2. Taking the triplet energy of **10**(U) as a reference, the energies of **11** and **12** are $J_3 = -2.88$ and $J_4 = +14.09$ kcal/mol, respectively, which will be used for the paramagnetism calculations. The energy order of these σ-dimers is $E(\mathbf{11}) \ll E(\mathbf{4}) < E(\mathbf{12})$, which appears to be correlated with the σ-bond lengths as can be seen in Figure 4. **11** and **4** are lower in energy than **12** because the σ-bonds for **11** and **4** are right next to the two etheno clamps. **4** is less stable than **11** simply because of the

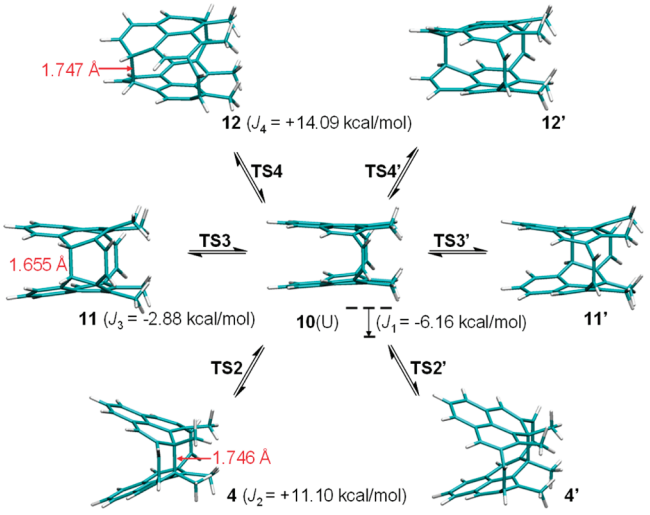

Figure 4. π-Dimer **10** of the boat conformation may undergo σ-dimerizations at the six pairs of spin-bearing α-C atoms, forming three unique σ-dimers (**4**, **11**, and **12**) that are connected to **10** by three corresponding transitions states (TS2−TS4). These structures and three other σ-dimers and three other transitions states form a pairwise relation where each pair is related by symmetry and is indicad by the same primed and unprimed symbol. Energies J_2 (also shown in Figure 2), J_3, and J_4 are relative to the triplet energy of **10**(U).

(41) Li, Y.; Lampkins, A. J.; Baker, M. B.; Sumpter, B. G.; Huang, J.; Abboud, K. A.; Castellano, R. K. *Org. Lett.* **2009**, *11*, 4314.

methyl clustering effects discussed above. It is noteworthy that with all these additional σ-dimers found, the global minimum of the boat conformation is still the π-dimer **10**(U) and therefore a Cope rearrangement still does not exist. However, **11** and **11′** are only 3.28 kcal/mol higher than the singlet of **10**(U) and these low-lying states may be significantly populated around room temperature.

Paramagnetic Susceptibilities. Because of the radical nature of the phenalenyl units, phenalenyl-derivatives exhibit interesting magnetic properties.[3,7,8,11,12] For the staggered π-dimer of **2**, SQUID measurements yielded a singlet−triplet energy difference of −6.64 kcal/mol obtained by fitting magnetic susceptibilities with the widely used Bleaney−Bowers dimer model.[11c] The paramagnetism comes from the triplet of the π-dimer since singlet states are magnetically silent. As can be seen from Figure 2, for **5**(U), there are two degenerate singlet states of σ-dimers, one singlet of the π-dimer, and its low-lying triplet. Similar to the Bleaney−Bowers model and on the basis of the van Vleck formula,[42] one may derive the equation containing all of the three singlet states and the low-lying triplet state

$$\chi T = \frac{2Ng^2\beta^2}{k[3+\exp(-J_1/kT)+2\exp(-J_2/kT)]} \quad (1)$$

where χ is the paramagnetic susceptibility, T is the absolute temperature, N is Avogadro's number, g is the gyromagnetic factor, β is the electronic Bohr magneton, and k is the Boltzmann constant. For **10**(U), as can be seen from Figures 2 and 4, there are six singlet states of σ-dimers, one singlet of the π-dimer, and its low-lying triplet. The corresponding equation contains all of the seven singlet states and the low lying triplet states

$$\chi T = (2Ng^2\beta^2)/(k\{3+\exp(-J_1/kT) + 2[\exp(-J_2/kT)+\exp(-J_3/kT)+\exp(-J_4/kT)]\}) \quad (2)$$

The energies of singlet σ- and π-dimers relative to the triplet π-dimers are $J_1 = -4.79$ and $J_2 = -8.03$ kcal/mol for the chair conformation, and $J_1 = -6.16$, $J_2 = +11.10$, $J_3 = -2.88$, and $J_4 = +14.09$ kcal/mol for the boat conformation. Using these parameters, the paramagnetic susceptibilities of both chair and boat conformations can be estimated.

The computed χT values of **3** and **4** are shown in Figure 5 as a function of T. For comparison we also show χT for the staggered π-dimer of **2** calculated by the Bleaney−Bowers model using the singlet−triplet energy difference of $J = -6.64$ kcal/mol.[11c] We found that the χT value of the chair conformation is negligible while the χT value of the boat conformation is comparable to that of the π-dimer of **2** around room temperature. Therefore, similar to the π-dimer of **2**, the boat conformation may exhibit paramagnetic properties, which may be observable by SQUID and/or solid state ESR, whereas the chair conformation has a very small magnetic response. We note that the different magnetic properties of the chair and boat conformations come directly from the different nature of the global minima.

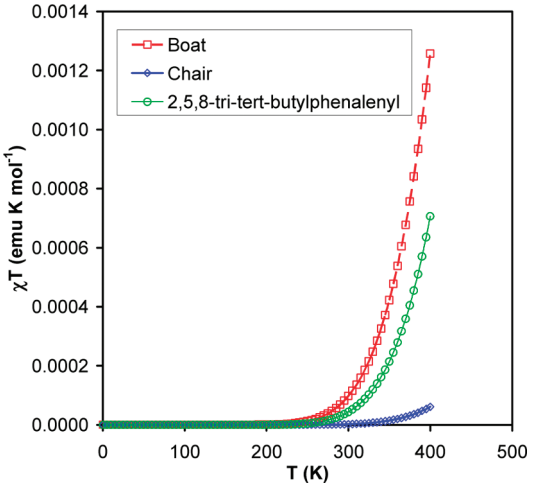

Figure 5. Calculated χT as a function of T for the chair and boat conformations of cyclo-biphenalenyl molecular materials using eqs 1 and 2, respectively, and for the π-dimer of 2,5,8-tri-*tert*-butylphenalenyl using the Bleaney−Bowers dimer model. Parameters for the calculations are discussed in the text.

Thermochromism. Morita et al. synthesized a diazaphenalenyl molecular material that was green and the color darkened with increasing temperature.[11c] Its reversible thermochromism can be ascribed to the tautomerizations between σ- and π-dimers.[8b,11c] In comparison, the staggered π-dimer of **2** shows a deep blue color but no thermochromism was reported.[12] It was also found that the title compound **3** forms yellow-orange needles. Obviously, the common feature of these phenalenyl derivatives is their electronic absorption in the visible part of the electromagnetic spectrum. In the following, we examine the UV−vis spectra of the chair and boat conformations of cyclo-biphenalenyl molecular materials using ZINDO/S calculations. We note that it is our group as well as others' experience that the ZINDO/S method is qualitatively good in reproducing UV−vis spectroscopic transitions when used with the CI singles method.[41,43,44]

The UV−vis transitions for the σ- and π-dimers of the title compounds with geometries from the RM06 optimizations are shown in Figure 6. It is straightforward to see that the σ-dimers only have UV absorptions (< 390 nm) while the π-dimers have electronic absorption in both the UV and visible (390−770 nm) ranges. Other σ-dimers for the boat conformation were also examined and no visible-range absorption was obtained. The visible-range absorptions for **5**(R) and **10**(R) are at 540 and 603 nm, respectively, both of which are due to the HOMO−LUMO transitions. The corresponding absorptions for **5**(U) and **10**(U) have wavelengths at 665 and 685 nm, respectively (see Figure S2 in the Supporting Information). These wavelengths are larger than those of **5**(R) and **10**(R), in agreement with the longer interphenalenyl distances from

(42) Kahn, O. *Molecular Magnetism*; VCH Publishers: New York, 1993; pp 5−7, 104.

(43) Risko, C.; Kushto, G. P.; Kafati, Z. H.; Brédas, J. L. *J. Chem. Phys.* **2004**, *121*, 9031.

(44) Gierschner, J.; Mack, H. G.; Oelkrug, D.; Waldner, I.; Rau, H. *J. Phy. Chem. A* **2004**, *108*, 257.

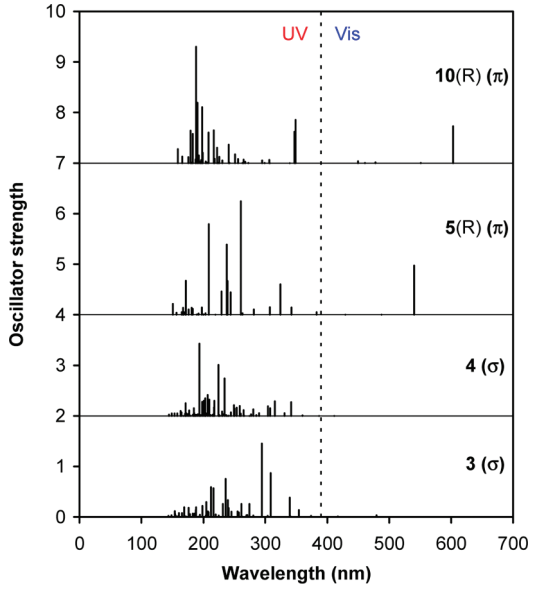

Figure 6. UV−vis spectra of the σ- and π-dimers (from the RM06 geometry optimizations) for the chair and boat conformations of cyclo-biphenalenyl molecular materials calculated using parametrized ZINDO/S theory.

the broken-symmetry calculations, which lead to weaker SOMO−SOMO couplings and smaller HOMO−LUMO gaps. These spectroscopic calculations indicate that the above-mentioned various colors of phenalenyl derivatives can be attributed to differences in the electronic transitions of the π-dimers vs the σ-dimers. Because the global minimum of the chair conformation is a doubly degenerate σ-dimer **3** and **3′**, the yellow-orange color found in the needle crystals of **3** may be explained by the population of the $\pi-\pi$ bonded intermediate **5** due to the dynamic equilibrium during the course of the Cope rearrangement. According to the Boltzmann distribution, one expects that the color of the chair conformation should darken with increasing temperature, similar to the experimental observation for the diazaphenalenyl.[11c] For the boat conformation, since the global minimum is the $\pi-\pi$ bonded structure, as temperature increases, the electronic structures of the degenerate σ-dimers will be increasingly populated at the cost of the π-dimer population, especially for **11** and **11′** that have the lowest energies among the σ-dimers. Therefore, it is expected that the color of the boat conformation will become lighter with increasing temperature. Together with the paramagnetism, these different physicochemical properties offer phenalenyl-derivatives the potential in applications such as "smart" π-functional materials.

To provide a unified DFT interpretation, we also performed TDDFT calculations. Similar to the ZINDO/S results, we did not find any prominent absorptions for the σ-bonded **3** or **4** in the visible range. In comparison, **5**(R) and **10**(R) have absorptions in the visible range at 729 and 705 nm, respectively, both coming from the HOMO−LUMO transitions. The corresponding absorptions for the UM06-based structures, i.e., **5**(U) and **10**(U), are at much greater wavelengths that sit at the border of near-infrared and visible ranges (see the Supporting Information). Nevertheless, these results support the ZINDO/S findings shown above. Comparing the TDDFT wavelength of 729 nm for **5**(R) with the ZINDO/S result of 540 nm, it is interesting to see that the ZINDO/S result is closer to the experimental wavelength around 580 nm as implied from the yellow-orange color of the chair conformation. This agrees with the consensus among the practitioners that ZINDO/S is a good choice for UV−vis calculations. The applicability of the ZINDO/S to these molecules under study is more or less unexpected since this level of theory is not parametrized for this new type of $\pi-\pi$ bonding (or weak bonds). We note that the head-over-head $\pi-\pi$ overlaps between π-stacked phenalenyl units shown in Figure 3 may be different from traditional orbital overlaps that can be found in many other unsaturated aromatic compounds. Specifically, the delocalized orbitals are somewhat like π-orbitals participating in $\sigma-\sigma$ overlaps.

4. Conclusions

In this paper, we have examined two cyclo-biphenalenyl biradicaloid molecular materials with chair and boat conformations. Calculations were carried out with restricted and broken-symmetry DFT using primarily the M06-class of meta-GGA functionals with occasional comparison to the most widely used B3LYP hybrid functional. We have found that the M06 hybrid meta-GGA is best suited for this category of compounds, giving molecular structures and reaction barriers that agree satisfactorily with experimental values. The valence tautomerizations and magnetic properties of the two conformations have been studied using the selected meta-GGA functional.

It is found that the chair conformation involves a 2e/4c $\pi-\pi$ bonded structure, whereas the boat conformation involves a 2e/12c $\pi-\pi$ bonded structure on their potential energy surfaces. Both structures were characterized by Mayer bond orders, showing that there are non-negligible bond orders at the overlapping carbon pairs, in agreement with the SOMO−SOMO electron pairings. NICS calculations produced strongly negative NICS values, indicative of the aromaticity of the phenalenyl π-dimer. We note that the aromaticity may come from the cagelike structure due to the head-over-head $\pi-\pi$ overlap of HOMO orbitals (Figure 3).

The chair conformation exhibits a stepwise [3,3]-sigmatropic rearrangement, via the 2e/4c $\pi-\pi$ bonded intermediate. However, the global minimum for the boat conformation is the $\pi-\pi$ bonded structure. These differences on the potential energy surface give rise to a negligible paramagnetic susceptibility around room temperature for the chair conformation. In comparison, the paramagnetic susceptibility of the boat conformation should be observable by SQUID and/or ESR. UV−vis electronic spectroscopy results obtained using parametrized theory and TDDFT indicate that the various colors of phenalenyl derivatives should come from the electronic transitions of the π-dimers. According to the difference of the global minima of the two conformations, it is expected that the color of the chair conformation would become darker, whereas that of the boat conformation would become lighter with increasing temperature.

Phenalenyl and its derivatives are intriguing types of molecular materials as a result of a 2e/mc $\pi-\pi$ bonding that

may compete with the slightly stronger stretched σ-bonds. It is worth pointing out that such $\pi-\pi$ bonding have been observed both experimentally and theoretically in even anionic or cationic π-radicals, such as TCNE,[14] TCNQ,[45] TCNP,[46] and TTF.[47] The bond fluctuation between the $\pi-\pi$ bonding and stretched σ-bonds may enable variations of physicochemical properties of these and similar molecular materials, giving "smart" π-functional materials that sense and react to environmental stimuli.

(45) (a) Garcia-Yoldi, I.; Miller, J. S.; Novoa, J. J. *J. Phys. Chem. A* **2009**, *113*, 7124. (b) Huang, J.; Kingsbury, S.; Kertesz, M. *Phys. Chem. Chem. Phys.* **2008**, *10*, 2625.
(46) Novoa, J. J.; Stephens, P. W.; Weerasekare, M.; Shum, W. W.; Miller, S. S. *J. Am. Chem. Soc.* **2009**, *131*, 9070.
(47) (a) Wang, F. F.; Wang, Y.; Wang, B. Q.; Wang, Y. F.; Ma, F.; Li, Z. R. *Sci. China, Ser. B: Chem.* **2009**, *52*, 1980. (b) Rosokha, S. V.; Kochi, J. K. *J. Am. Chem. Soc.* **2007**, *129*, 828. (c) Garcia-Yoldi, I.; Miller, J. S.; Novoa, J. J. *J. Phys. Chem. A* **2009**, *113*, 484. (d) Halling, M. D.; Bell, J. D.; Pugmire, R. J.; Grant, D. M.; Miller, J. S. *J. Phys. Chem. A* **2010**, *114*, 6622.

Acknowledgment. Research at the Center for Nanophase Materials Sciences (CNMS) at Oak Ridge National Laboratory was sponsored by the Scientific User Facilities Division, U.S. Department of Energy (user project CNMS2010-232 to MK). The authors at Georgetown University thank the U.S. National Science Foundation for its support of the research at Georgetown University. We are grateful to Drs. R. J. Harrison and E. Apra for the discussions and help with broken symmetry calculations in NWChem and to Prof. D. J. Tantillo for the insightful discussions on Cope rearrangements.

Supporting Information Available: Thermodynamic data for the calculations of Table 2, clustering effects of methyl groups in **4**, derivation of the rate constant for a degenerate stepwise reaction, HOMOs of broken-symmetry π-dimers **5**(U) and **10**(U), locations for NICS calculations, UV−vis spectra for π-dimers with geometries from UM06 optimizations, TDDFT calculated UV−vis absorptions, Cartesian coordinates of all structures, and full author list of refs 21, 22, and 28 (PDF). This material is available free of charge via the Internet at http://pubs.acs.org.